DECELERATION OF A POROUS ROTATING DISK IN A VISCOUS FLUID

Layne T. Watson
Kishore Kumar Sankara
Luegina Mounfield

CS83029-R

DECELERATION OF A POROUS ROTATING DISK IN A VISCOUS FLUID

LAYNE T. WATSON*

Department of Computer Science
Virginia Polytechnic Institute and State University
Blacksburg, VA 24061
U.S.A.

KISHORE KUMAR SANKARA

Department of Mathematics
Indian Institute of Technology
Madras 600036, India

LUEGINA MOUNFIELD

Department of Computer Science
University of Florida
Gainesville, FL 32601
U.S.A.

ABSTRACT

The flow due to a rotating disk decelerating with an angular velocity inversely proportional to time with either surface suction (or injection) which again varies with time is investigated. The unsteady Navier-Stokes equations are transformed to non-linear ordinary differential equations using similarity transformations. The resulting equations are solved numerically using a globally convergent homotopy method. The flow depends on two non-dimensional parameters, namely an unsteadiness parameter S and a suction (or injection) parameter A. Some interesting numerical results are presented graphically and discussed.

---

*This work was supported in part by NSF Grant MCS 8207217.

1. INTRODUCTION

Von Karman [1] noted first that the governing Navier-Stokes equations for the steady viscous flow over an infinitely large rotating disk reduced to self similar forms and obtained approximate solutions. Later Cochran [2] calculated more accurate solutions to the above problem by numerical integration of the equations.

The fluid rotation is essentially unsteady at the start of the motion before attaining the steady state. Hence there was much interest in this transient phase of flow. Thriot [3] investigated the problem of flow due to a suddenly accelerated or stopped disk. Nigam [4] discussed the flow and pressure function in the early stages of motion for the suddenly accelerated motion of a viscous incompressible fluid. The case of unsteady motion of a viscous liquid around a gradually rotating disk with the angular velocity assumed to be time-dependent was solved by Dolidge [5]. Sparrow and Gregg [6] investigated the flow about a disk rotating unsteadily with time varying angular velocity. Benton [7] discussed the steady state problem and investigated the flow due to a suddenly accelerated disk. Chawla [8] studied the change from one steady state rotation (von Karman solution) to a slightly faster steady state rotation. All these problems are based on perturbation series. Rath and Iyengar [4] studied in detail, by the Galerkin method, the unsteady flow produced by a porous rotating disk with time dependent angular and suction (or injection) velocities.

Problems are found in the literature where the time-dependent Navier-Stokes equations admit similarity solutions. Some of these problems are the unsteady stagnation point flow found by Yang [10], the squeezing of a fluid between circular or two dimensional plates by Wang [11], the squeezing of a fluid filled tube by Uchida and Aoki [12], and deceleration of a rotating disk in a viscous fluid by Watson and Wang [13].

In this paper we study the deceleration of a porous rotating disk where the angular and suction (or injection) velocities are taken to be time dependent.

This difficult non-linear two point boundary value problem is integrated numerically by a new homotopy method developed by Watson [14]. The method has been successfully used for several non-linear two point boundary value problems by Wang and Watson [15], [16], and was found to converge where other standard methods diverge. The homotopy method converges regardless of the starting point, and thus is truly globally convergent.

2. FORMULATION

We use cylindrical polar coordinates, r, θ, z and denote the corresponding velocity components by u, v, w. The disk surface occupies the plane $z = 0$ and rotates about

the z-axis. In accordance with Watson and Wang [13], we use the following transformations

$$u = \frac{\Omega_o r}{(1-\alpha t)} f'(\eta) \qquad .. (1)$$

$$v = \frac{\Omega_o r}{(1-\alpha t)} g(\eta) \qquad .. (2)$$

$$w = \frac{-2(\nu \Omega_o)^{1/2}}{(1-\alpha t)^{1/2}} f(\eta) \qquad ..((3)$$

$$p = -\frac{\rho \nu \Omega_o}{(1-\alpha t)} P(\eta) \qquad .. (4)$$

where p is the pressure, ρ is the density, ν is the kinematic viscosity and

$$\eta = \left(\frac{\Omega_o}{\nu}\right)^{1/2} \frac{z}{(1-\alpha t)^{1/2}} \qquad .. (5)$$

Here the angular velocity of the disk $\Omega(t)$ and suction (or injection) velocity $W(t)$ are taken as

$$\Omega(t) = \Omega_o/(1-\alpha t) \qquad .. (6)$$

and

$$W(t) = -\sqrt{\nu \Omega_o}\, A / (1-\alpha t)^{1/2} \qquad .. (7)$$

α and A are constants and Ω_o is a positive constant. $A > 0$ corresponds to suction and $A < 0$ to injection.

Using (1) - (5), the unsteady Navier-Stokes equations [13] reduce to a set of non-linear ordinary differential equations

$$f'''+2ff''+g^2-f'f' = S(\tfrac{1}{2}\eta f''+f') \qquad ..(18)$$

$$g''-2f'g+2fg' = S(\tfrac{1}{2}\eta g'+g) \qquad ..(9)$$

where $S = \alpha/\Omega_o$ is a non- dimensional number measuring unsteadiness, and primes denote differentiation with respect to η.

The boundary conditions are

$$\begin{aligned} f(0) &= A, \quad f'(0) = 0, \quad g(0) = 1 \\ f'(\infty) &= 0, \quad g(\infty) = 0 \end{aligned} \qquad ..(10)$$

3. METHOD OF SOLUTION

Equations (8) - (10) are solved using the globally convergent homotopy algorithm [14] which does not require a good initial approximation. The method is described briefly as follows:

$$\text{Let} \quad \underset{\sim}{V} = \begin{pmatrix} f''(0) \\ g'(0) \end{pmatrix} \qquad ..(11)$$

and

$$\underset{\sim}{F}(\underset{\sim}{V}) = \begin{pmatrix} f'(T;\ \underset{\sim}{V}) \\ g\ (T;\ \underset{\sim}{V}) \end{pmatrix} = \underset{\sim}{0} \qquad ..(12)$$

where T is sufficiently large such that

$$f(T) \approx f(\infty), \quad g(T) \approx g(\infty)$$

Define $\underset{\sim}{\phi}_{\underset{\sim}{a}} : [0,1) \times E^n \longrightarrow E^n$ by

$$\underset{\sim}{\phi}_{\underset{\sim}{a}}(\lambda, \underset{\sim}{V}) = \lambda \underset{\sim}{F}(\underset{\sim}{V}) + (1-\lambda)(\underset{\sim}{V}-\underset{\sim}{a}) \qquad ..(13)$$

The earlier work of Chow et.al.[17] and Watson [14] showed that for almost all $\underset{\sim}{a}$ (in the sense of Lebesgue measure) the zero set of $\underset{\sim}{\phi}_{\underset{\sim}{a}}$ in $[0,1) \times E^n$ contains a smooth curve γ emanating from $(0,\underset{\sim}{a})$, and the Jacobian matrix $D\underset{\sim}{\phi}_{\underset{\sim}{a}}$ has full rank along γ (even if γ turns). Under certain hypotheses on $\underset{\sim}{F}(\underset{\sim}{V})$, γ reaches a zero $\bar{\underset{\sim}{V}}$ of $\underset{\sim}{F}$ at $\lambda = 1$. This amounts to solving the initial value problem

$$\frac{d}{ds}\underset{\sim}{\phi}_{\underset{\sim}{a}}(\lambda(s), \underset{\sim}{V}(s)) = \underset{\sim}{0}, \quad \lambda(0) = 0 \qquad ..(14)$$

$$||(\lambda(s), \underset{\sim}{V}(s))|| = 1, \quad \underset{\sim}{V}(0) = \underset{\sim}{a} \qquad ..(15)$$

where s is arc length along γ (see [14] for the practical implementation of the homotopy algorithm).

4. CONCLUSIONS

In the case of axial distribution of velocity, positive values indicate an inflow towards the disk from the free stream while negative values indicate an outward flow towards the free stream. For different values of the unsteady parameter S

the axial distribution is presented in Figures (6,9) for injection and Fig. (3) for suction. When suction is applied the axial velocity at infinity towards the disk is larger than for the impermeable disk (Watson and Wang [13]). From Fig. (3) it can be seen that as the magnitude of S increases the flow at infinity also increases. In the case of injection, Figures (6,9), the incoming stream is retarded by the outflowing stream of injected fluid. The greater the injection velocity the more strongly the inflow is opposed. Hence there is a decrease in the magnitude of the axial flow at infinity with increased injection velocity. As the injection velocity increases the outflow penetrates to greater distances from the disk surface. As a result the crossover point between the negative and positive axial velocity is pushed farther outward. The same phenomenon is observed by increasing the magnitude of S.

The above discussion is reflected by the radial velocity distribution given in the Figures (1,4,7). When suction is applied, Fig. (1), the radial velocity decreases and the maximum occurs at smaller η , as compared to the impermeable case (Ref. [13]). The radial velocity increases with increase in the magnitude of S. The level of the radial velocity is raised with an increase in injection velocity and an increase in magnitude of S. This can be seen from Figures (4,7). From the Figures (1,4,7) it can be observed that the boundary layer becomes thinner and more prominent for large negative S.

The tangential velocity distribution can be seen from the figures (2,5,8). In the case of suction ($A = 1,0$), fig. (2), for $S < S^* = 8.6292$ and in the case of injection ($A = -2$), Fig. (5), for $S < S^* = 1.256461$ and ($A = -.5$), fig. (8), for $S < S^* = -.865099$, the fluid near the disk rotates faster than the disk. This is attributed to the fact that for fast deceleration of the disk (more negative S) the fluid rotation is unable to decay as fast as the disk. Fluid deceleration near the disk surface is faster in the case of suction while it is slower in the case of injection. Table 2 gives the values of S for different A's for which $g'(0) = 0$.

Neglecting the edge effects we may write the torque experienced by a disk of large but finite radius R as

$$T = -2\pi \int_0^R r^2 \rho \nu \left(\frac{\partial v}{\partial z}\right)_{z=0} dr$$

$$= -\frac{1}{2} \pi R^4 (\nu \Omega_o^3)^{1/2} (1 - \Omega_o St)^{-3/2} g'(0)$$

When $0 \geq S > S^*$, the rotating disk experiences a resistance since $g'(0)$ is negative, while for $S < S^*$, the disk experiences a torque in the direction of rotation as $g'(0)$ is positive. Table 1 gives the values of $g'(0)$ for different values of S and A. For $0 \geq S > S^*$, for all A, the magnitude of the resistance experienced by the disk reduces for decreasing S,

and for $S < S^*$ the torque experienced by the disk increases for decreasing S. The particular interesting case of $S = S^*$ corresponds to the decay of rotation of a free, massless disk in an infinite fluid.

REFERENCES

[1] T. VON KARMAN, Z. Angew. Math. Mech., 1, 233 (1921).

[2] W. G. COCHRAN, Proc. Camb. Phil. Soc., 30, 365 (1934).

[3] H. K. THRIOT, Z. Angew. Math. Mech., 20, 1 (1940).

[4] S. D. NIGAM, Q. Appl. Math., 9, 89 (1951).

[5] D. E. DOLIDGE, Prikl. Mat. Mech., 18, 371 (1954).

[6] E. M. SPARROW and J. I. GREGG, J. Aeronaut. Sci., 27, 252 (1960).

[7] E. R. BENTON, J. Fluid Mech., 24, 781 (1966).

[8] S. S. CHAWIA, J. Fluid Mech., 78, 609 (1976).

[9] R. S. RATH, and S.R.K. IYENGAR, Nat. Inst. of Sci. of India Proc., 35, 180 (1969).

[10] K. T. YANG, J. Appl. Mech., 25, 421 (1958).

[11] C. Y. WANG, J. Appl. Mech., 43, 579 (1976).

[12] S. UCHIDA and H. AOKI, J. Fluid Mech., 82, 371 (1977).

[13] L. T. WATSON and C. Y. WANG, Phys. Fluids, 22, 2267 (1979).

[14] L. T. WATSON, Appl. Math. Comp., 5, 297 (1979).

[15] C. Y. WANG and L. T. WATSON, Z. Agnew. Math. Phys., 30, 195 (1979).

[16] C. Y. WANG and L. T. WATSON, Appl. Sci. Res., 35, 195 (1979).

[17] S. N. CHOW, J. MALLETT - PARET and J. A. YORKE, Math. Comp., 32, 887 (1978).

FIGURE CAPTIONS

Figure 1. Radial flow velocity distribution $f'(\eta)$ for A = 1.0 and S = -20, -10, -5, -2, -1, -.5, 0.0 (top to bottom).

Figure 2. Tangential flow velocity distribution $g(\eta)$ for A = 1.0 and S = -20, -10, -5, -2, -1, -.5, 0.0 (top to bottom).

Figure 3. Axial flow velocity distribution $f(\eta)$ for A = 1.0 and S = -20, -10, -5, -2, -1, -.5, 0.0 (top to bottom).

Figure 4. Radial flow velocity distribution $f'(\eta)$ for A = -.2 and S = -20, -10, -5, -2, -1, -.5, 0.0 (top to bottom).

Figure 5. Tangential flow velocity distribution $g(\eta)$ for A = -.2 and S = -20, -10, -5, -2, -1, -.5, 0.0 (top to bottom).

Figure 6. Axial flow velocity distribution $f(\eta)$ for A = -.2 and S = -20, -10, -5, -2, -1, -.5, 0.0 (top to bottom).

Figure 7. Radial flow velocity distribution $f'(\eta)$ for A = -.5 and S = -20, -10, -5, -2, -1, -.5, 0.0 (top to bottom).

Figure 8. Tangential flow velocity distribution $g(\eta)$ for A = -.5 and S = -20, -10, -5, -2, -1, -.5, 0.0 (top to bottom).

Figure 9. Axial flow velocity distribution $f(\eta)$ for A = -.5 and S = -20, -10, -5, -2, -1, -.5, 0.0 (top to bottom).

S \ A	-.5	-.2	0.0	1.0	3.0	5.0
0.0	.489480 -.302172 (13.5)	.516445 -.468360 (13.5)	.510225 -.615917 (10.0)	.242416 -2.038526 (9.0)	.083298 -6.001541 (9.0)	.049997 -10.000333 (9.0)
-.5	.603523 -.129177 (10.0)	.630690 -.285914 (10.0)	.614283 -.428406 (10.0)	.256255 -1.919949 (7.0)	.083876 -5.959905 (4.0)	.050122 -9.975335 (4.0)
-1.0	.731015 .048379 (9.0)	.750622 -.098044 (9.0)	.719787 -.236575 (10.0)	.270049 -1.801463 (7.0)	.084454 -5.918269 (4.0)	.050247 -9.950338 (4.0)
-2.0	1.008138 .416866 (8.0)	.997706 .289219 (7.0)	.931507 .154981 (10.0)	.297524 -1.564717 (6.0)	.085609 -5.834996 (4.0)	.050497 -9.900342 (4.0)
-5.0	1.911857 1.593348 (5.0)	1.756017 1.501086 (5.0)	1.562797 1.360850 (10.0)	.379293 -.855807 (5.0)	.089075 -5.585181 (4.0)	.051247 -9.750357 (4.0)
-10.0	3.495329 3.672101 (4.0)	3.029122 3.594832 (4.0)	2.600801 3.413860 (10.0)	.514195 .322887 (4.0)	.094852 -5.168828 (4.0)	.052496 -9.500380 (4.0)
-20.0	6.743608 8.011314 (4.0)	5.572189 7.889504 (4.0)	4.646424 7.579882 (10.0)	.781166 2.674404 (4.0)	.106405 -4.336139 (4.0)	.054996 -9.000429 (4.0)

TABLE 1. f"(0), g'(0), and T (where f(T) ~ f(infinity)) .

A	S	f"(0)
-.5	-.865099	.695641
-.2	-1.256461	.813327
0.0	-1.606699	.848244
1.0	-8.629200	.477339

TABLE 2. S and f"(0) for which g'(0) = 0 .

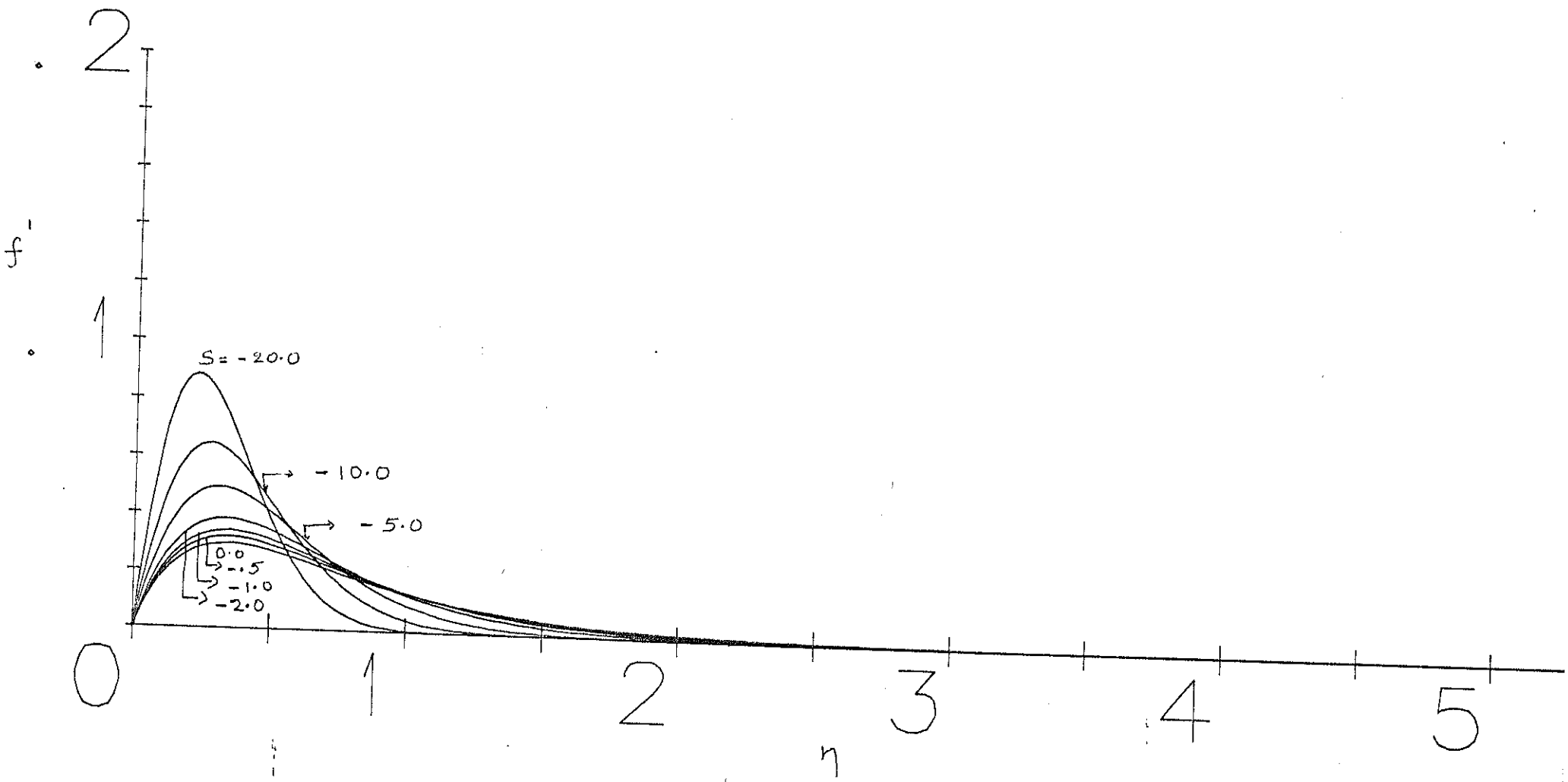

Figure : 1

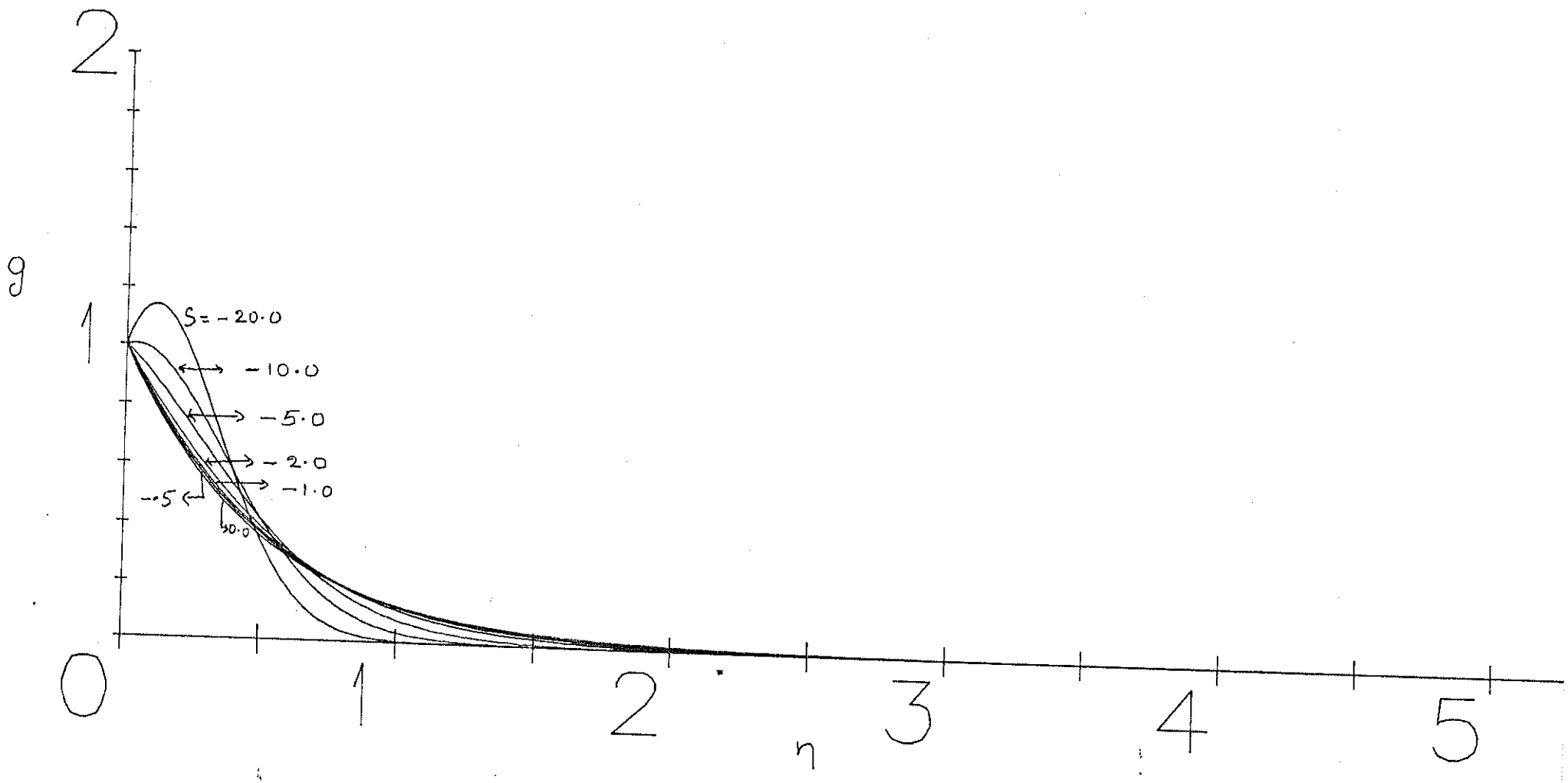

Figure : 2

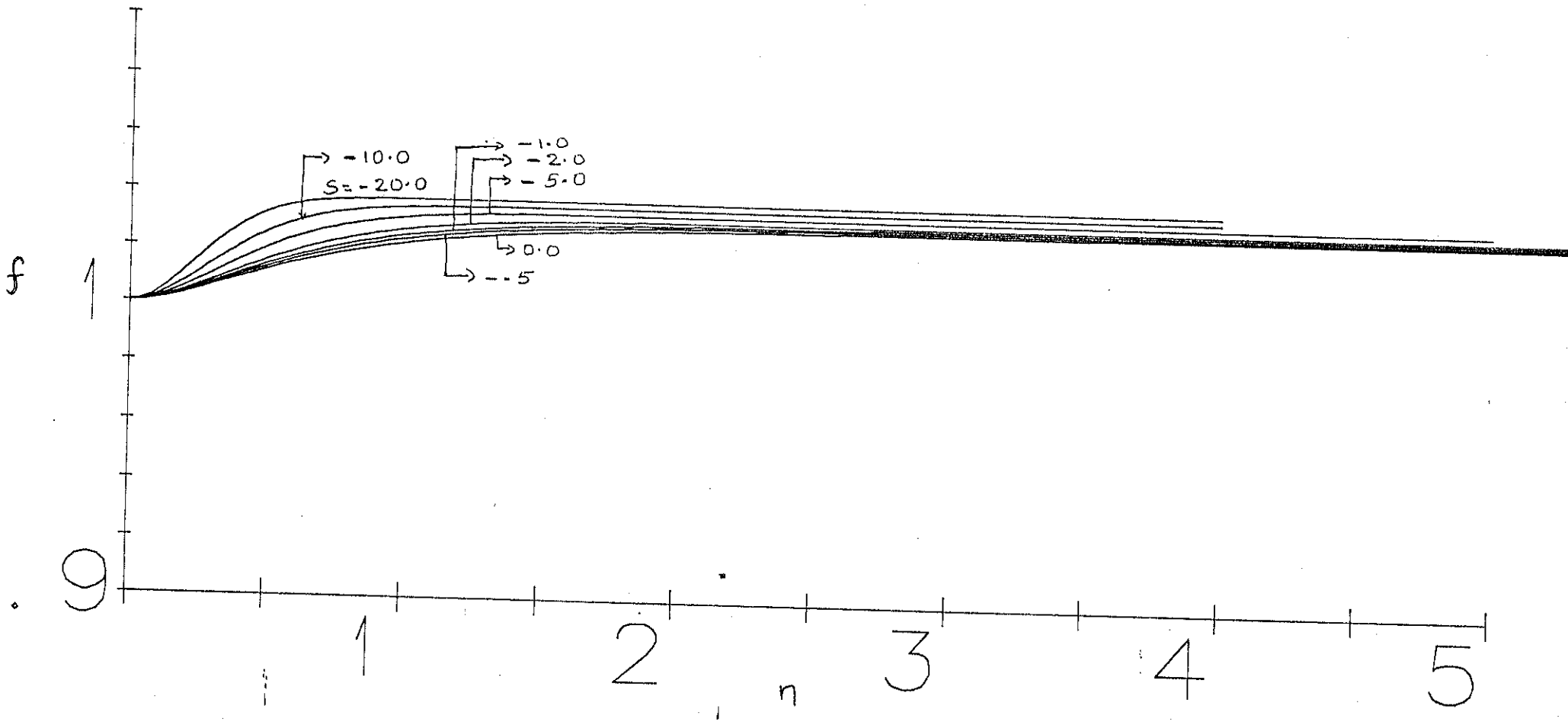

Figure : 3

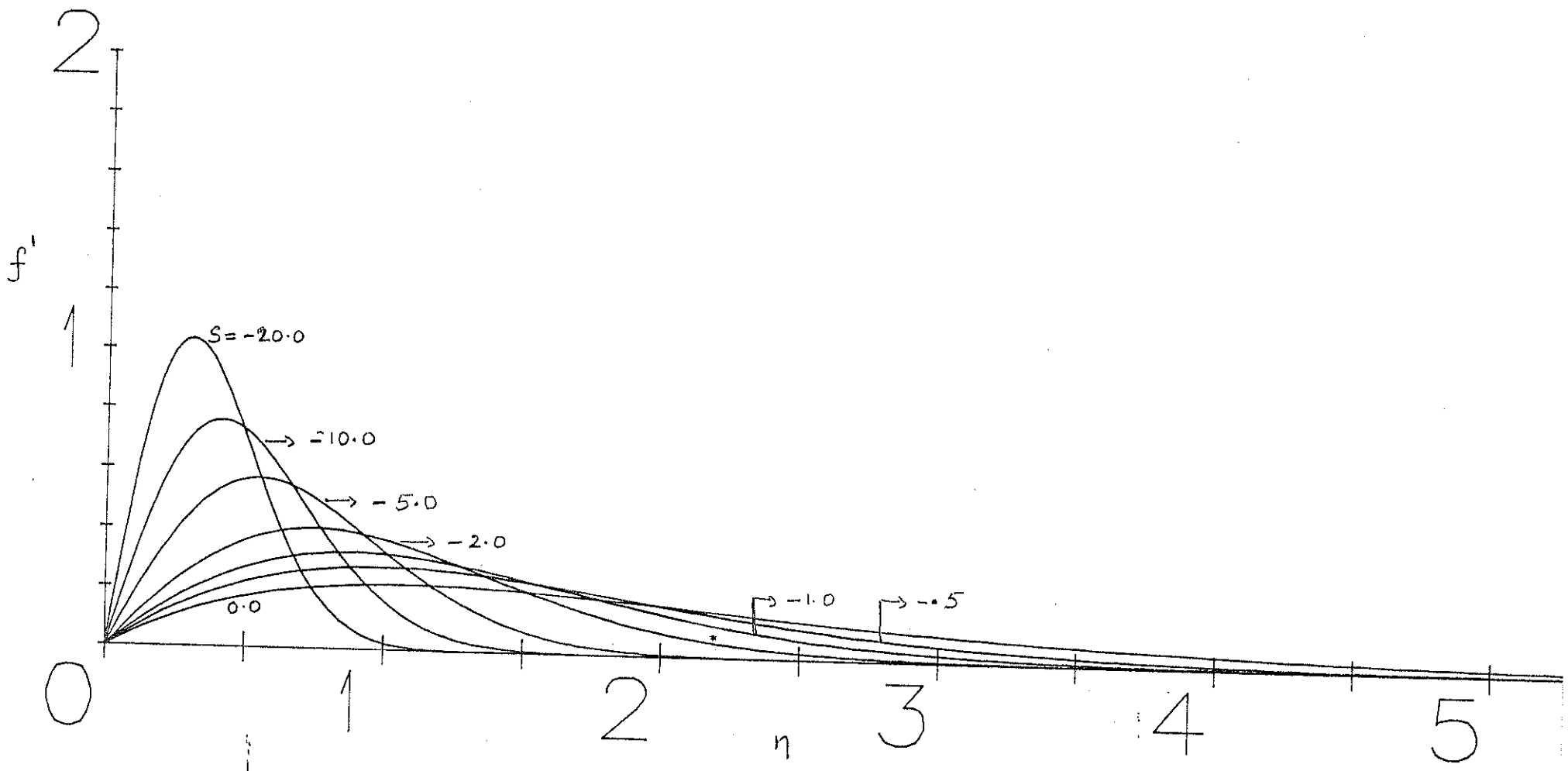

Figure : 4

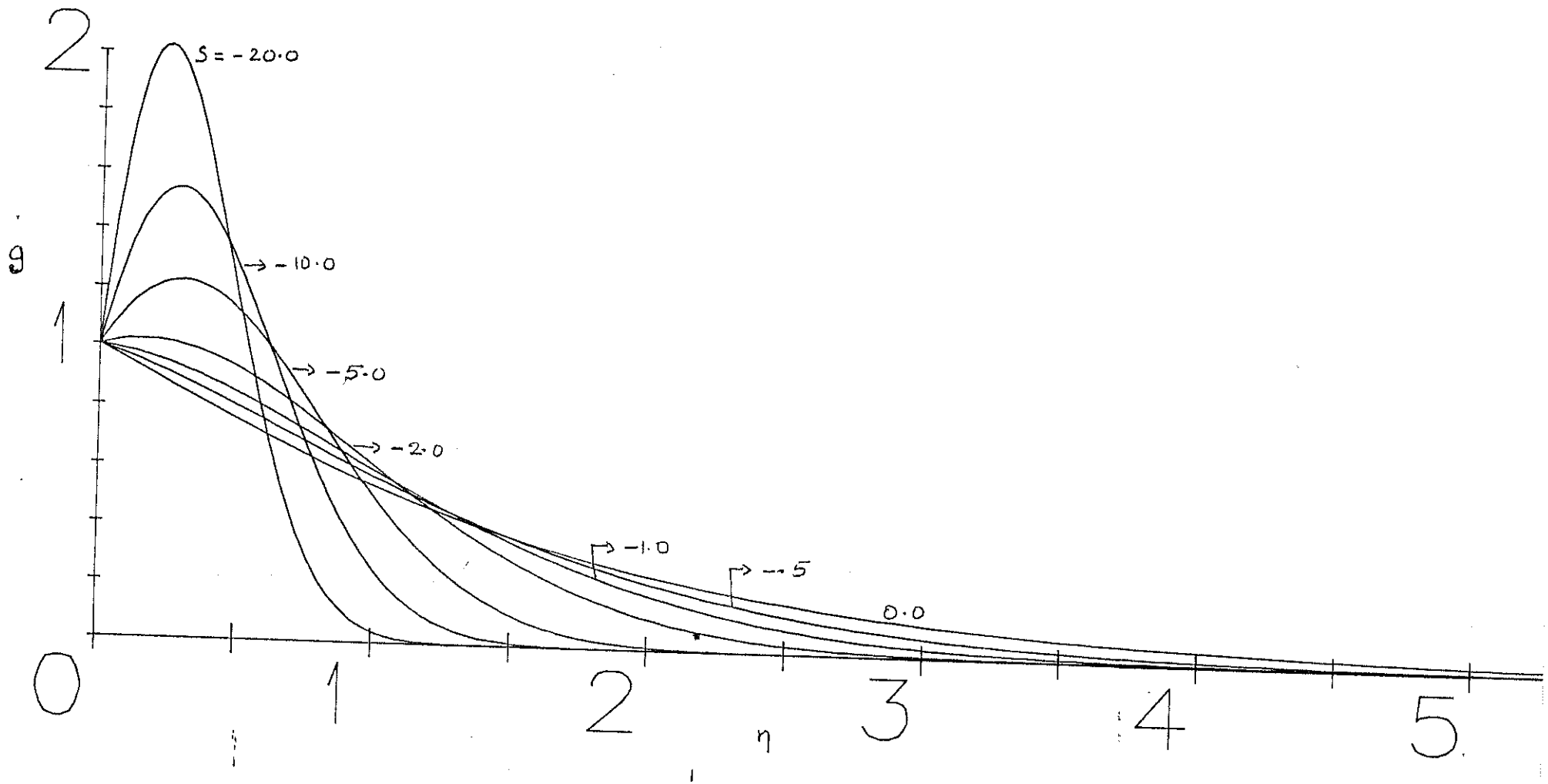

Figure : 5

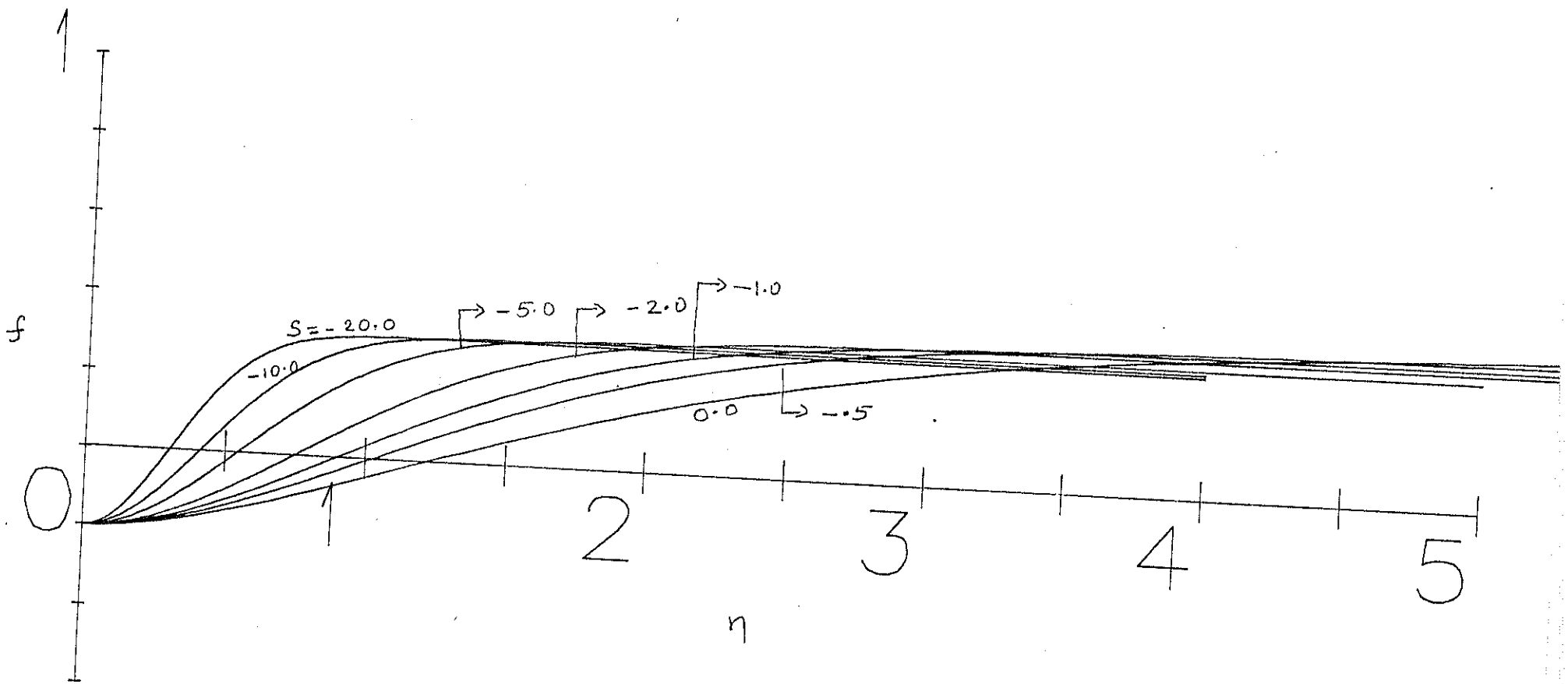

Figure : 6

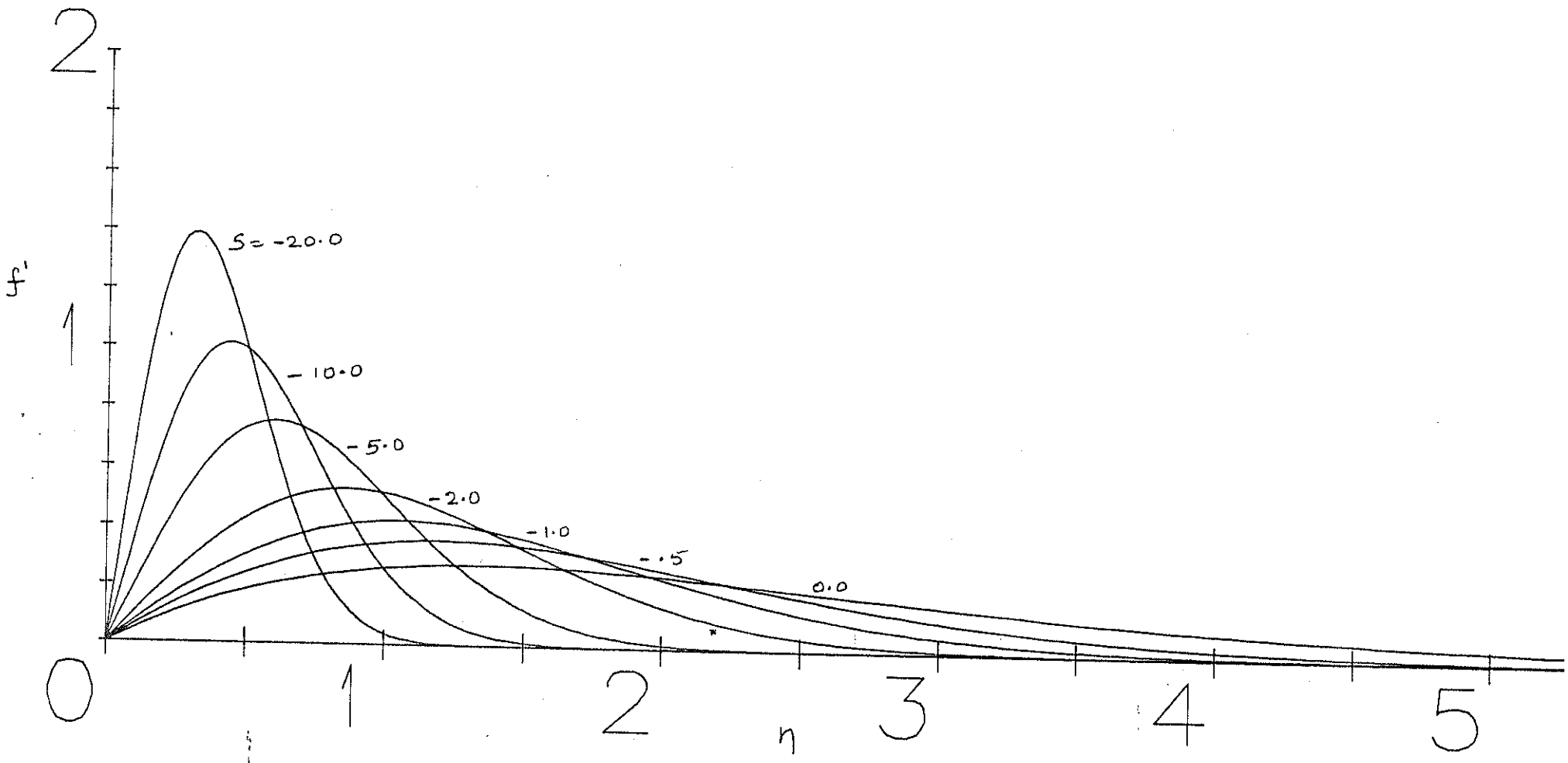

Figure : 7

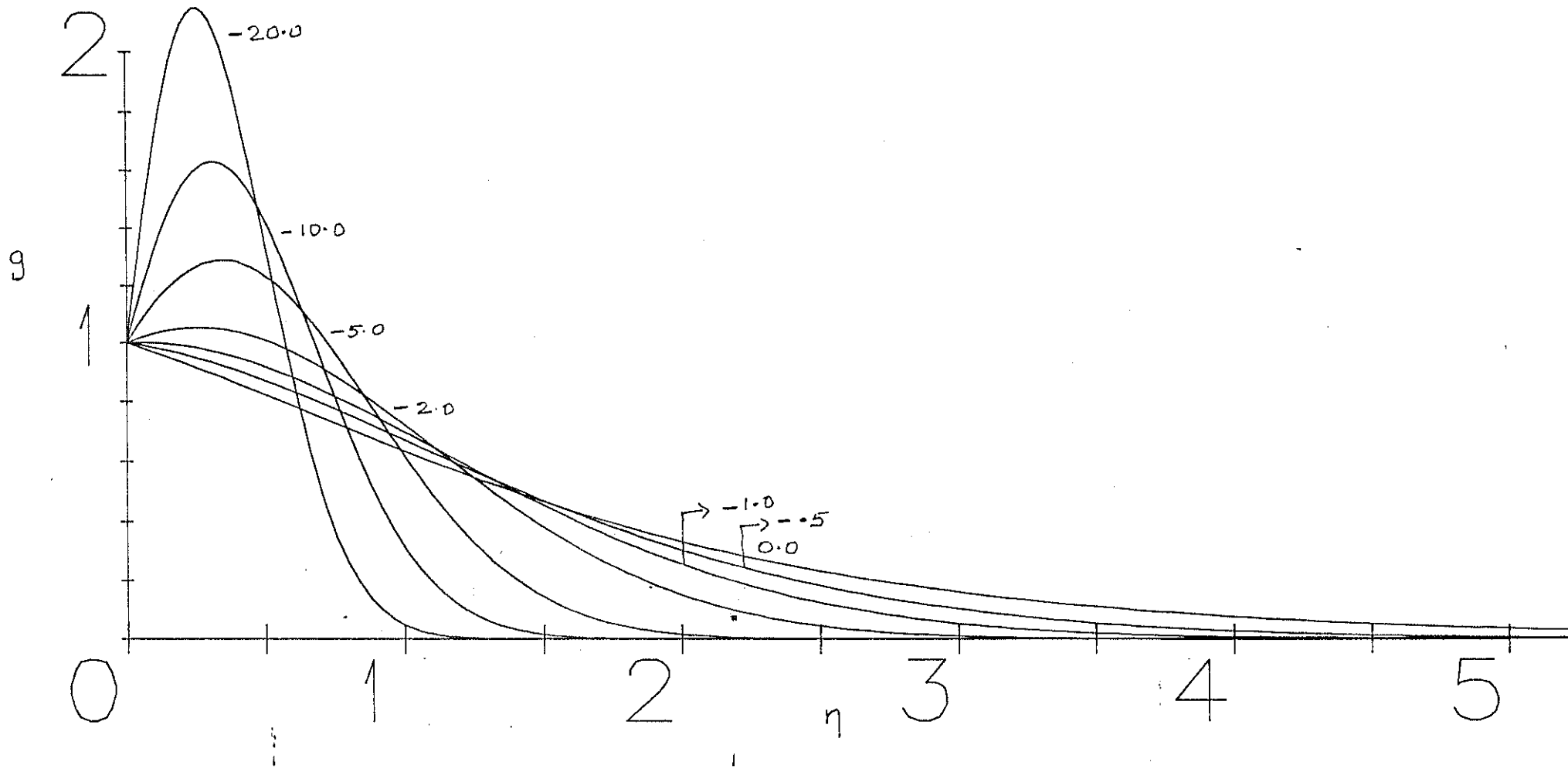

Figure: 8

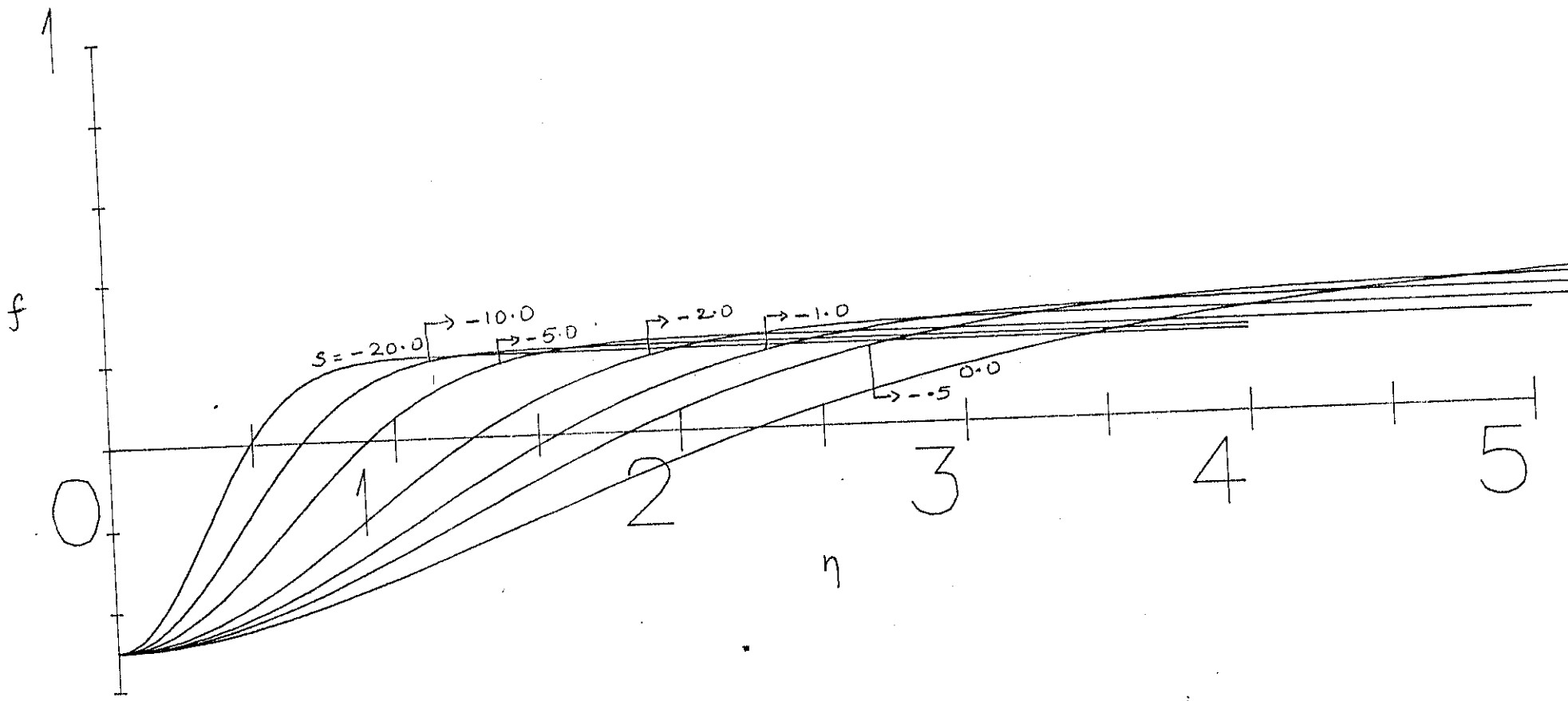

Figure : 9